Determination of the Threshold for Instability in Four-Wave Mixing Mediated by Brillouin Scattering

D. E. WATKINS, ANDREW M. SCOTT, AND KEVIN D. RIDLEY

Abstract—**The threshold for instability in Brillouin-enhanced four-wave mixing has been experimentally determined as a function of both the phase mismatch and the ratio of the pump beam intensities, and is shown to agree with theoretical modeling. The effective input noise intensity for four-wave mixing in the unstable regime is compared to the noise in a stimulated Brillouin scattering amplifier and is found to be higher by a factor of three in the forward direction. Competition between two input signals has been investigated and it is shown that the signal which arrives first dominates the interaction in the unstable regime.**

Introduction

FOUR-WAVE mixing mediated by Brillouin scattering has been shown to result in very high reflectivity phase conjugation. This results from an instability in Brillouin-enhanced four-wave mixing (BEFWM), which causes both the transmitted signal and the phase conjugate beam to grow rapidly until pump depletion sets in [1]–[7]. The instability occurs when the pump beams exceed a threshold intensity that depends on the ratio of the two pump beam intensities and on the phase mismatch. In this paper, we present results of experimental studies confirming theoretical predictions for the dependence of the threshold intensity in BEFWM on both the phase mismatch and the ratio of the pump beam intensities. We also discuss the competition between the signal and noise, and between two signals, in BEFWM.

Review of Theory

Theoretical analysis of BEFWM has been treated previously [2], [6], [8]. We will briefly review the theory in a simplified form following the analysis given in [6]. In conventional stimulated Brillouin scattering, an acoustic wave is driven by electrostriction in the moving interference field formed by a pump beam and its Stokes wave. In BEFWM there are two interference terms that drive an acoustic wave, the first is the interference between one pump beam and its Stokes beam, and the second is between the other pump beam and its anti-Stokes beam (assuming that any frequency difference that exists between the pump beams is not resonant with the Brillouin medium, or is decoupled from the SBS medium through opposite polarization of the pump beams). We will consider the case of a signal which is Stokes-shifted with respect to the stronger pump beam [5] rather than anti-Stokes shifted [1]–[4], [6], [7] (see Fig. 1). The acoustic wave is described by the solution of the equation

$$(1 + ix)u + \frac{1}{\delta\omega_0}\frac{\partial u}{\partial t} = -\beta\left\{E_2^* E_3 + E_1 E_4^* \exp(i\Delta kz)\right\} \tag{1}$$

where E_1 is the field of the stronger pump beam, E_2 is the field of the weaker pump beam, E_4 is the field of the Stokes beam, and E_3 is the field of the anti-Stokes beam. In the case of an anti-Stokes signal, the input boundary condition is given by $E_3(z = 0, t)$, while in the case of a Stokes signal the input is given by $E_4(z = L, t)$. In either case an acoustic wave is formed which travels counter to the weaker pump beam. The stronger pump beam is Stokes scattered into E_4 while the weaker beam is anti-Stokes scattered into E_3. The notation used here is that of [6]. The only difference is that we now solve for a Stokes input signal instead of an anti-Stokes input. In (1), β is the electrostrictive coupling parameter, and $x = \delta\omega/\delta\omega_0$ is the normalized detuning of the signal wave from resonance, where $\delta\omega = \omega_1 - \omega_4 - \omega_s$, ω_s is the Brillouin resonance frequency, $\delta\omega_0 = 1/2\tau_B$, and τ_B is the phonon lifetime. We use the usual definition of the phonon lifetime as the decay of the acoustic intensity [9] rather than the acoustic amplitude [10]. Note that the frequencies of the four waves are related by energy conservation in the

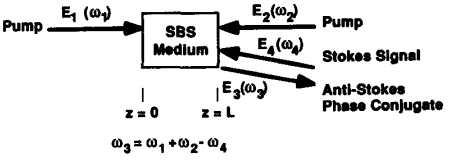

Fig. 1. Diagram of four-wave mixing interaction. In our experiments, the angle between the pump beams and the signal beam was <3 mrad, so the interaction was essentially colinear.

Manuscript received September 14, 1989; revised July 25, 1990. The research described in this work was performed at the Royal Signals and Radar Establishment under the auspices of the U.K. Ministry of Defence and the U.S. Department of Energy.

D. E. Watkins is with the Los Alamos National Laboratory, Los Alamos, NM 87545 and was on change of station at the Royal Signals and Radar Establishment, Malvern, Worc. WR14 3PS, England.

A. M. Scott and K. D. Ridley are with the Royal Signals and Radar Establishment, Malvern, Worc. WR14 3PS, England.

IEEE Log Number 9040278.

four-wave mixing process, $\omega_3 = \omega_1 + \omega_2 - \omega_4$. The phase mismatch is $\Delta k = k_1 - k_2 - k_3 + k_4$ in the nearly colinear geometry used here.

Assuming undepleted pump beams, the equations for the electric fields are given by

$$\frac{\partial E_3}{\partial z} = \frac{g}{2\beta} E_2 u \tag{2a}$$

$$\frac{\partial E_4}{\partial z} = \frac{g}{2\beta} E_1 u^* \exp(i\Delta k z). \tag{2b}$$

In these equations, g is the Brillouin gain coefficient.

These equations can be solved to find a steady-state reflectivity by setting the time derivative in (1) to zero [11]. However, above the threshold for instability, this steady-state solution is not valid. In the unstable regime, the acoustic wave will grow rapidly in time until pump depletion occurs. The reflectivities obtained in this regime can be much greater than those predicted by the steady state solution.

To analyze the transient behavior we assume that the pump beams are constant throughout the interaction, and that the input signal beam is a step function in time. Clearly such an approach cannot be used to predict the reflectivity after pump depletion sets in. However, useful information about the threshold for the instability and the rate of growth of the instability can be found. Taking Laplace transforms of (1) and (2) gives

$$\frac{\partial \bar{E}_3}{\partial z} = \frac{g}{2\beta} E_2 \bar{u} \tag{3a}$$

$$\frac{\partial \bar{E}_4^*}{\partial z} = \frac{g}{2\beta} E_1^* \bar{u} \exp(-i\Delta k z) \tag{3b}$$

$$\bar{u} = \frac{-\beta\delta\omega_0}{[s + \delta\omega_0(1 + ix)]} \left\{E_2^* \bar{E}_3 + E_1 \bar{E}_4^* \exp(i\Delta k z)\right\} \tag{3c}$$

where the bar denotes the Laplace transform, and s is the Laplace transform conjugate variable of t. Substituting from (3c) into (3a) and (3b) gives

$$\frac{\partial \bar{E}_3}{\partial z} = -h\left[|E_2|^2 \bar{E}_3 + E_1 E_2 \bar{E}_4^* \exp(i\Delta k z)\right] \tag{4a}$$

$$\frac{\partial \bar{E}_4^*}{\partial z} = -h\left[|E_1|^2 \bar{E}_4^* + E_1^* E_2^* \bar{E}_3 \exp(-i\Delta k z)\right] \tag{4b}$$

where

$$h = \frac{g\delta\omega_0}{2\{s + \delta\omega_0(1 + ix)\}}.$$

These equations can be decoupled into linear second-order equations and solved. Assuming that the Stokes signal is a step function at $t = 0$, the boundary conditions are

$$E_4(L, t) = E_{40} H(t) \Rightarrow \bar{E}_4(L, s) = \frac{E_{40}}{s}$$

and

$$E_3(0, t) = 0 \Rightarrow \bar{E}_3(0, s) = 0. \tag{5}$$

Here, L is the length of the interaction zone. This leads to a solution for the output phase conjugate and amplified signal of the form

$$\bar{E}_3(L, s) = \frac{-2hE_1E_2E_{40}^* \exp(i\Delta k L)}{s^*\left\{h\left[|E_2|^2 - |E_1|^2\right] + i\Delta k + \chi \coth\left[\frac{\chi L}{2}\right]\right\}} \tag{6a}$$

$$\bar{E}_4^*(0, s) = \frac{\chi E_{40}^* \exp\left\{\frac{hL}{2}\left[|E_1|^2 + |E_2|^2\right] + i\frac{\Delta k L}{2}\right\}\left\{\sinh\left[\frac{\chi L}{2}\right]\right\}^{-1}}{s^*\left\{h\left[|E_2|^2 - |E_1|^2\right] + i\Delta k + \chi \coth\left[\frac{\chi L}{2}\right]\right\}} \tag{6b}$$

where the complex variable

$$\chi^2 = \left\{h\left[|E_1|^2 + |E_2|^2\right] - i\Delta k\right\}^2 + 4ih\Delta k|E_2|^2.$$

We note that both h and χ are functions of s. The time dependence is then given through the inverse transforms of (6).

In general, the inverse Laplace transform does not lead to an analytic expression for $E_3(L, t)$. However, (6a) and (6b) provide useful information about the behavior of the BEFWM process. Both fields are functions of the complex variable s and these functions have a common series of poles; one for $s = 0$ and an infinite number associated with the cyclic nature of the complex hyperbolic cotangent function. We denote these poles as s_{pn}. Applying the residue theorem, each pole will contribute to the inverse transform of the Stokes and anti-Stokes fields, leading to solutions of the form

$$E_3(L, t) = \sum_{n=-\infty}^{\infty} a_n \exp(s_{pn} t) + b \tag{7a}$$

$$E_4(0, t) = \sum_{n=-\infty}^{\infty} c_n \exp(s_{pn} t) + d \tag{7b}$$

where the a_n and c_n are associated with the coth function, and b and d correspond to $s = 0$.

If the real part of any of the poles is positive, exponential growth of the waves E_3 and E_4 will result. The con-

ditions for which this applies can be ascertained by examining the nature of the poles in (6a) and (6b). The behavior of the output fields given in (7a) and (7b) will be dominated by one or two poles which have real parts significantly larger than the others. The imaginary part of the pole corresponds to a frequency shift in the scattered light. In [2] it is shown that the pole with the largest growth rate will also be the pole with a frequency shift that brings the interaction closest to resonance.

The poles s_{pn} depend on the following five variables: the Brillouin linewidth $\delta\omega_0$; the sum of the normalized pump intensities $M = M_1 + M_2$; the ratio of the pump intensities a; the phase mismatch ΔkL; and the normalized detuning x. Here, we have introduced the dimensionless variables

$$M_1 = g|E_1|^2 L, \quad M_2 = g|E_2|^2 L, \quad \text{and } a = \frac{M_2}{M_1}. \tag{8}$$

For fixed values of ΔkL and a, the poles s_{pn} of (6) and (7) correspond to fixed values of $h(s_{pn})|E_1|^2$. This leads to the relation

$$\text{Re}\,(s_{pn}) = \delta\omega_0 \left[\frac{M}{M_{\text{crit}}} - 1\right] \tag{9a}$$

where M_{crit} is the critical or threshold intensity for exponential growth for the pole, and depends only on a and ΔkL. The corresponding imaginary part is

$$\text{Im}\,(s_{pn}) = \frac{M}{M_{\text{crit}}}\,\text{Im}\,(s_c) + \delta\omega_0 \left[\frac{M}{M_{\text{crit}}} - 1\right] x \tag{9b}$$

where Im (s_c) is the imaginary part of the pole at the critical intensity.

The critical intensity can be obtained for given values of a and ΔkL by 1) selecting an arbitrary value of M, 2) using M, a, and ΔkL to find the zeros s_{pn} for the denominators of (6), and 3) using (9) to determine M_{crit}. Such calculations were presented in [2] and [6]. From these references, there appears to be no limit to the size of the phase mismatch. Indeed, a limitation on phase mismatch does exist, but is so large as to be inconsequential. To determine this limit, we note that there are two sets of interference fringes with wave vectors $\boldsymbol{k}_{s1} = \boldsymbol{k}_1 - \boldsymbol{k}_4$ and $\boldsymbol{k}_{s2} = \boldsymbol{k}_3 - \boldsymbol{k}_2$, We have assumed that the acoustic waves with these wave vectors have the same acoustic frequency. This is clearly valid only when $|k_{s1} v_s - k_{s2} v_s| < \delta\omega$, or equivalently $\Delta kL < L/\alpha_s$, where α_s is the acoustic decay length. This still allows for very large phase mismatches ($\Delta kL < 10^4$ to 10^5) for realistic geometries. The principle of conservation of momentum is not violated, since the phonons are continually decaying and in the overall process both energy and momentum are transferred from the optical beams into the bulk of the nonlinear medium.

The presence of some phase mismatch appears to be a necessary feature of the instability. The FWM process provides a feedback mechanism into the acoustic wave throughout the interaction length. If the process were simply the Stokes scattering of one beam and the anti-Stokes scattering of another beam with perfect phase matching, then the feedback of the anti-Stokes process would be negative (that is removing power from the acoustic wave) and no instability would develop. However, in the presence of a large enough phase mismatch the anti-Stokes process can provide positive feedback and the instability will develop. This happens at the cost of reduced anti-Stokes output intensity [2]. We note that even in the case of zero applied phase mismatch, the instability can develop because the frequency offset in the transient response [see (9b)] creates the required phase mismatch.

In the remainder of this paper, our objective is to compare our experimental measurements to the theoretical results of [2] and [6].

Experimental Approach

A diagram of our experiment is given in Fig. 2. The basic four-wave mixing arrangement consists of two counterpropagating pump beams, both circularly polarized with the same handedness in the interaction region. The signal beam E_4 was injected at an angle of <3 mrad to the axis, but with opposite handedness to the pump beams, and so interacts in the Brillouin medium with the counterpropagating pump beam E_1. The second pump beam E_2 was scattered to form the phase conjugate wave E_3. The use of circularly-polarized light in the Brillouin interaction facilitated the separation of the signal beams from the pump beams. The pump beam E_1 was obtained directly from the amplified laser output and so was at the frequency $\omega_1 = \omega_L$. The other pump beam E_2, was generated by SBS from the first pump beam in cell 2, and had a frequency determined by the Brillouin medium in this cell, $\omega_2 = \omega_L - \omega_{SBS2}$. The signal beam was obtained by Brillouin scattering in cell 4, and had a frequency $\omega_4 = \omega_L - \omega_{SBS4}$. The frequencies of the pump beam 2 and the signal beam 4 were tuned either by changing the temperature of the Brillouin medium for small-frequency tuning (for most liquids, $\Delta\upsilon/\Delta T \approx 10$ MHz/°C, see [10]), or by changing the Brillouin medium for larger tuning. In SBS cell 2, we used mixtures of CS_2 and CCl_4 in various proportions to obtain frequency shifts over the range of 2.7 to 3.7 GHz. The four-wave mixing medium was $TiCl_4$, which has a frequency shift of 3.07 GHz. This material was also used to generate the signal beam 4. We measured a temperature tuning coefficient of 9.6 MHz/°C for this material, so that a $\sim 20°$ temperature change results in a tuning of almost the full linewidth of 200 MHz.

The intensity of the pump beam 1 was varied by using a $\lambda/2$ plate between two polarizers. This gave a dynamic range of $>200:1$ in intensity. The relative intensity of pump beam 2 to pump beam 1 was set by adjusting the $\lambda/4$ wave plate before SBS cell 2 for a specific value of $a = I_2/I_1$. Since SBS in this cell was highly saturated, the ratio stayed fixed as the intensity of pump beam 1 is varied.

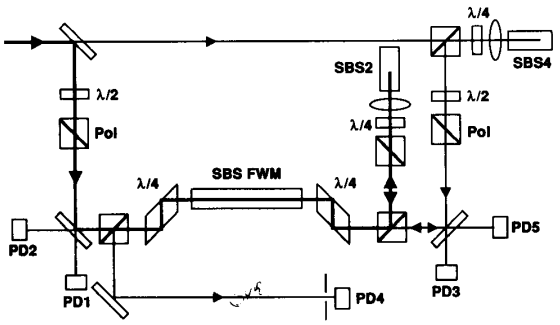

Fig. 2. Schematic diagram of the experimental arrangement. Fresnel rhombs were used to generate circularly polarized pump and signal beams in the four-wave-mixing (FWM) cell. This facilitates separation of the beams. Pump beam 1 enters the FWM cell from the left, and is phase-conjugated in a simple lens plus SBS cell (SBS2) to generate pump beam 2. The signal beam 4 is derived through SBS in cell SBS4, and injected into the FWM cell from the right at an angle of <3 mrad to the pump. $TiCl_4$ was used in the FWM and SBS4 cells, while mixtures of CS_2 and CCl_4 were used in the SBS2 cell. Signals were monitored by photodiodes PD1–5.

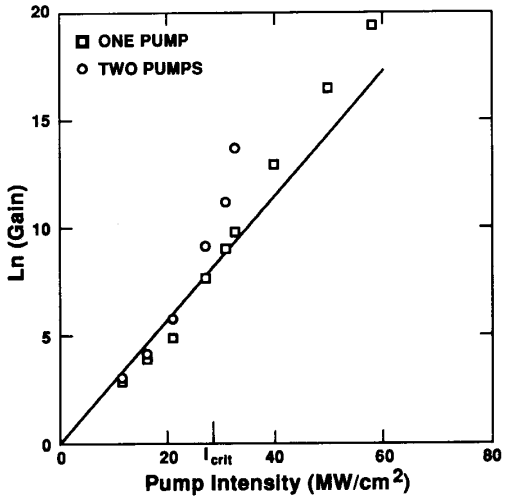

Fig. 3. Forward signal gain as a function of pump intensity in the presence of one (squares) and two (circles) pump beams. The threshold intensity for the instability occurs when the amplified signal with two pump beams is significantly greater than the amplified signal with one pump beam. The theoretical value for the threshold is labeled I_{crit}.

Experimental Results

Initially, we characterized the SBS interaction by measuring the gain for a resonant signal as a function of the intensity of pump beam 1 (blocking pump beam 2). We calibrated the photodiode monitoring pump beam 1 by measuring the energy through a 0.9 mm diameter pinhole as a function of the integrated photodiode signal. The ratio of the integrated photodiode signal to the peak signal gave an effective laser pulse duration for calculating peak intensities. In our case, this value was 24 ns, which was also the full width at half maximum for our pulse. The amplified signal as a function of pump intensity for SBS in $TiCl_4$ is shown in Fig. 3. The slope of this curve is equal to the gain coefficient g times the length of the interaction medium L, giving $g = 0.015$ cm/MW. This agrees with the value given in [9]. Also shown in Fig. 3 is the amplification of the signal with both pump beams present. Below the threshold for the instability, the presence of the second pump beam has only a slight effect on the output signal. The threshold for the instability is seen as the slight increase in output at the highest intensities. When the pump intensity was increased above this point, the output signal went off scale in this plot.

For the data of Fig. 3, the second pump beam was obtained using a mixture of 80% CS_2: 20% CCl_4 with a measured frequency shift relative to $TiCl_4$ of 430 MHz. We determined all the frequency shifts by constructing a modified Michelson interferometer, where the retroreflecting mirrors were the Brillouin cells [10]. This same approach was used to determine the temperature dependence of the frequency shift in $TiCl_4$. By observing the beat frequency in the output of the interferometer, a direct measurement of the frequency shift is obtained.

The phase mismatch for BEFWM is a function of the frequency of pump beam 2 and the cell length, and can be written as

$$\Delta kL = \frac{2nL}{c}\left|\omega_{SBS2} - \omega_{SBS4}\right| \tag{10}$$

where $n = 1.57$ is the index of refraction of the four-wave mixing medium. Measurements of the threshold for the instability were carried out using four mixtures in SBS cell 2, and using different FWM-cell lengths. The combined results are shown in Fig. 4. This figure also shows a theoretical curve for the threshold intensity as a function of phase mismatch (see [2], [5], and [6]). Note that each pole s_{pn} has an associated threshold intensity. This plot gives the minimum threshold intensity for a given value of ΔkL. Thus the maxima correspond to points where two poles have the same critical intensity.

For a given cell length, the relative critical intensity as a function of ΔkL can be determined to within 5%. The absolute critical intensities depend on accurate calibration of the pump intensity, which could be determined to within 10%. The experimental points are displaced from the theoretical curve by a constant factor of 1.3. This is the result of the finite duration of our laser pulse, which requires that the rate of growth be fast enough so that the effect of the instability appears before the pump pulse falls below the critical intensity. The amplification of the signal intensity due to the instability is given by

$$G_{inst} = \exp\left\{\frac{t_p}{\tau_B}\left(\frac{M}{M_{crit}} - 1\right)\right\}$$

where t_p is the pulse length. The amplification of the input signal by pump beam 1 alone is simply

$$G_{amp} = \exp\left(gI_1L\right)$$

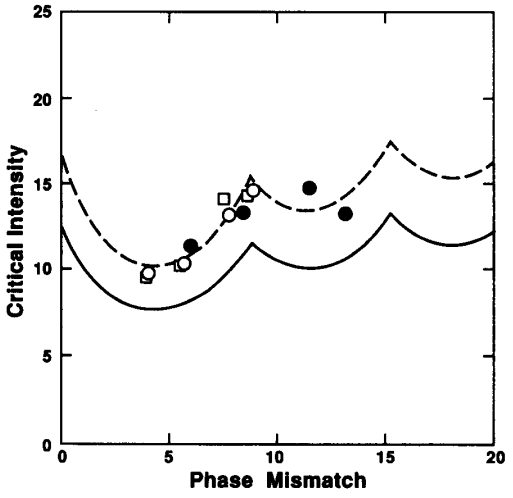

Fig. 4. Comparison of experimentally determined normalized threshold intensity (M_{crit}) with theoretical model. The solid curve is the model for a step function input, and the dashed curve is simply a factor of 1.3 times the solid curve (see text). The data were taken in three different cell lengths: 20 cm (open circles), 19.6 cm (squares), and 29.6 cm (filled circles). For each cell length the phase mismatch ΔkL was varied by changing the SBS medium for pump beam 2.

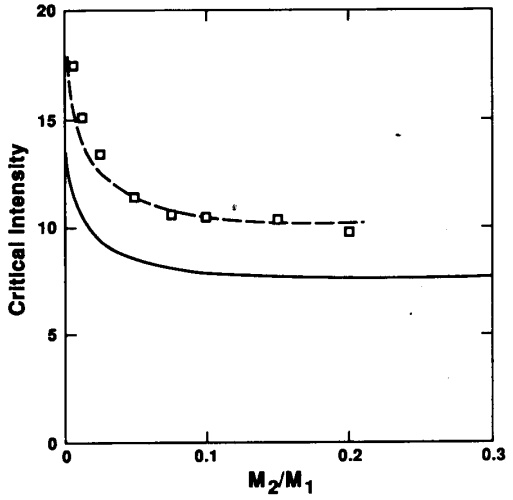

Fig. 5. Experimental and theoretical normalized instability threshold intensity (M_{crit}) as a function of pump intensity ratio, $a = M_2/M_1$. The dashed curve is once again a factor of 1.3 times the solid curve, which is determined for a step function input.

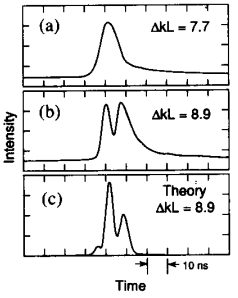

Fig. 6. (a) Typical output signal pulse for phase mismatch far from a maximum on the M_{crit} versus ΔkL curve (Fig. 4). (b) Modulated output pulse shape for $\Delta kL = 8.9$, near the maximum in Fig. 4. (c) Output pulse shape given by computer model simulating experimental conditions.

for steady-state amplification. (Steady state will be reached in a time $t \approx gILt_B = 7.5$ ns, which is shorter than our 24 ns FWHM pump pulse.) In our experiments we measured $gI_1L = 10$. We expect the amplification due to the instability to be observable only when $(t_p/\tau_B)(M/M_{crit} - 1) > 10$. For our pulse duration, $t_p/\tau_B = 33$, so the instability is observed for $M > 1.3M_{crit}$.

We also measured the threshold intensity as a function of the ratio of the intensity of pump beam 1 to pump beam 2 for constant phase mismatch ($\Delta kL = 5.7$). This is plotted in Fig. 5. The critical intensity has a broad minimum in the vicinity of $a = 0.1$, and grows rapidly as a is decreased. Our experimental value for the threshold intensity is again a factor of 1.3 times the theoretical prediction over a large range in pump beam ratio.

We commented above that the peaks in the theoretical curves of Fig. 4 occur when two poles of (6) have the same real parts. This implies that both poles will have the same growth rate and contribute equally to the amplified signal and phase conjugate. However, the two poles will generally have different imaginary parts, and therefore different frequency shifts during the transient growth of the amplified signal. This difference in frequency shift results in intensity modulation. Computer modeling suggests that this modulation will continue from the transient growth phase into the saturation regime [6]. We observed modulation in the amplified signal for phase mismatch near the maximum in Fig. 4. In Fig. 6(a), we show a typical pulse shape for the amplified signal. In Fig. 6(b), we show the pulse shape observed for $\Delta kL = 8.9$ (open circle in Fig. 4). Similar shapes were observed for the point in Fig. 4 at $\Delta kL = 8.7$ (square in Fig. 4), but not at $\Delta kL = 8.5$ (filled circle in Fig. 4). This pulse consists of two peaks separated by 7.1 ns with a modulation depth of more than 50%. We have used our computer model to predict the pulse shape of the amplified beam using the experimental parameters corresponding to Fig. 6(b). The result is shown in Fig. 6(c). This pulse is qualitatively similar to that in Fig. 6(b), with two main peaks separated by 6.4 ns. There were no free parameters in this model. The model predicts that some modulation should be seen within a range of $(\Delta kL)_{max} - 0.5 < \Delta kL < (\Delta kL)_{max} + 0.5$, where $(\Delta kL)_{max}$ is the value of the phase mismatch at the maximum. This range depends somewhat on the amount the pump intensity exceeds the threshold intensity for instability. We did not observe such a broad feature. However, there is some uncertainty in our determination of ΔkL, which depends primarily on the determination of the frequency of the second pump beam (see above). We esti-

mate this uncertainty to be $\sim 15\%$, which might explain why the modulation was not seen for the $\Delta kL = 8.5$ case. It should also be noted that as ΔkL is changed and the signal intensity varied, the theory (and model) predicts that the depth of modulation will change but the modulation frequency remains the same to within 10%.

Noise Characteristics

The issue of noise in Brillouin amplifiers and four-wave mixing systems has been treated by Bespalov *et al.* [5] and Matveev [12]. In a Brillouin amplifier, the noise results from spontaneously scattered pump radiation. This scattered radiation is amplified by essentially the same factor as an external signal. Thus the noise signal measured by detector PD4 in Fig. 1 with only pump beam 1 present is the gain G times an equivalent input noise intensity. This equivalent input noise intensity is determined by the number of thermally-excited acoustic phonons which can spontaneously scatter the pump beam into the detector's field of view, and can be estimated using a semiclassical argument. There will be $kT/h\nu_a$ phonons per transverse mode within a frequency bandwidth $\Delta\nu$; and $\pi\theta^2/4\lambda^2$ is the number of transverse phonon modes which can scatter light from the pump beam into the aperture of the photodetector. Each thermal phonon which scatters light into the signal path is equivalent to a noise photon so the equivalent noise power for an amplifier is [5], [12]

$$I_{\text{noise}} = \frac{\nu_s}{\nu_a} kT\,\Delta\nu\,\frac{\pi\theta^2}{4\lambda^2}. \tag{11}$$

In this expression, k is the Boltzman constant and T is the temperature, so $kT = 4 \times 10^{-21}$ J; the ratio of the Stokes frequency to the acoustic frequency is $\sim 10^5$; $\Delta\nu = 200$ MHz is the Brillouin linewidth; $\theta = 1.8$ mrad is the angle subtended by the aperture of photodiode 4; and $\lambda = 1\ \mu$m is the optical wavelength. Experimental determinations of the noise intensity agree with this estimate to within an order of magnitude [5], [13]. The measurement of the noise is sensitive to the precise determination of the gain. In our experiments, these measurements could generally be made only at high gain, $G \approx 10^8$. This requires $gIL \approx 19$. Thus a 10% uncertainty in pump intensity or g will result in factors of ~ 7 in the gain G, and hence in the determination of the effective input noise from the noise measured by PD1.

The noise in BEFWM results fundamentally from the same source. However, two additional factors are present. First, the instability causes the noise to grow in time at the same rate as a signal, until pump depletion sets in. Second, the scattering of pump beam 2 to generate the phase conjugate occurs with a relative efficiency determined by the phase mismatch and ratio of pump beam intensities. Thus the right-hand side of (11) should be multiplied by a correction factor of $\phi(\Delta k, a) \approx 1$ for our experimental conditions appears (see [5], [12], [14]). A detailed derivation of the parameter ϕ is outside of the scope of this paper, but its existence cannot be neglected. Physically, ϕ is dependent upon the relative scattering efficiency for the two pump beams, and describes the degree of correlation and the localization of the noise source. When $\phi \approx 1$ the system behaves as if there were a single noise source localized in a small region of space, in the same way as conventional SBS can be regarded as a high-gain amplifier with a noise source at one end (the treatment we used above for noise in an SBS amplifier). In this case, the effective noise can be predicted by semiclassical arguments based on the energy density of thermally excited phonons, the bandwidth, and the number of modes which can scatter light into the relevant solid angle. The extra mathematical complexity of assuming distributed and uncorrelated noise sources does not influence the result. In addition, the scattering efficiencies for the Stokes and anti-Stokes processes are approximately equal. However, when $\phi < 1$ the uncorrelated and distributed nature of the noise source does effect the scattering process, and the intensity component of the acoustic noise which contributes to the output is smaller (by a factor of ϕ) than one would predict using the semiclassical argument. This occurs only for small phase mismatch, $\Delta kL < \pi$, and large pump beam intensity ratios, $a > 0.2$. In our experiments $\phi \approx 1$.

We have measured the noise in BEFWM using CS_2 to generate pump beam 2 (so $\Delta kL = 8.7$). Without pump beam 2 present, we set pump beam 1 to give a gain of $G = 6 \times 10^7$, and injected a signal to obtain a signal-to-noise ratio of S/N = 15. With pump beam 2 present, the signal to noise measured at detector 4 was S/N = 5, or a factor of ~ 3 worse. The phase conjugate had S/N $\approx$ 1. Clearly the presence of two pump beams resulted in a degradation of the signal-to-noise. Theoretically we predict the fundamental noise level to be the same for the Brillouin amplifier and for both amplification and conjugation by FWM through SBS, and we do observe that they are equal within a factor of 15. Bespalov *et al.* [5] observed a slightly better signal-to-noise ratio for SBS FWM than for amplification. The differences between these results are due to slight differences in the experimental geometry and approach rather than any fundamental inconsistency. In both our work and that of Bespalov [5] the measured noise levels are as much as an order of magnitude greater than predicted by theory (the same is true for [15]).

The source of the additional noise in our experiment may be the second pump beam itself. Light from this source may be added to the signal through imperfect polarization decoupling. We have measured the gain of a signal generated in CS_2 and amplified using $TiCl_4$. The difference in frequency shift for these two media is 670 MHz, much greater than the 100 MHz half width of the $TiCl_4$ Brillouin shift. For a Lorentzian line, one would expect the gain to scale as $g(\nu) = g_0/(1 + \Delta\nu^2/\Delta\nu_0^2) \approx g_0/46$. Thus at our maximum pump intensity, where $g_0IL = 20$, one would expect $gIL = 0.43$ and $G = 1.5$. Ex-

perimentally, gains of $G \approx 2$ are observed, and the output signal is modulated at the beat frequency between the two SBS media, 670 MHz. Thus it appears that some of the additional noise in our BEFWM experiment may derive from the SBS cell used to generate pump beam 2, and that some of this noise is near resonance for the four-wave mixing process.

Additional sources of system noise have been identified. For example, imperfections in optics allow some of the pump beams to leak through polarizers, which combined with weak forward scattering (by dust, etc.) can superimpose unwanted light onto the path of the signal or conjugate beams resulting in increased system noise [15], [16]. A noise source which must be avoided is parasitic oscillation between surfaces at either end of the SBS FWM cell [17].

In BEFWM there is a direct competition between the noise and an input signal, which is not necessarily the case in a Brillouin amplifier. This is because the instability in BEFWM drives the process to saturation of the pump beams independent of the signal strength, whereas a Brillouin amplifier can be operated in a small signal regime without pump depletion. The presence of pump depletion means that the noise can be suppressed in the presence of a strong signal. This has been observed experimentally. The degree of suppression is related to the strength of the input signal and the arrival time of the signal [3]. It also depends on the ratio of the pump intensity to the critical intensity, which determines the degree of pump depletion.

Competition Between Two Signals

In [6] the response of BEFWM to sudden changes in the phase of the input signal was investigated through computer modeling. This model showed that once the instability was established, it was self-sustaining and impervious to changes in the phase of the input signal. The phase conjugate pulse was affected only when the phase shift occurred within a narrow time window during the growth of the instability. We have extended this computer modeling to investigate the effect of changes in the signal intensity. These results predict that, once the instability is established, the output does not respond to changes in the input signal intensity. Even switching the input signal to zero had no effect, and the conjugate intensity continued to grow until the pumps were depleted.

To investigate the response of BEFWM to a change in input signal, we injected a second signal into the four-wave mixing cell. This signal was delayed relative to the first signal by about 8 ns, and separated from the other signal and the pump by a small angle. The output intensity of the second signal was determined in the absence of the first signal. Then the intensity of the first signal was adjusted without the second signal present so that the output intensity equaled that observed for the second signal. When both signals were injected, the intensity of the second output signal was reduced by a factor of 5 relative to that observed without the first signal, whereas the intensity of the first signal was unaltered. This experiment was carried out just above threshold for the instability, where only $\sim 1\%$ of the pump beam was coupled into the signal. This ensured that noise did not build up to a significant level before the second signal arrived, and also minimized the effect of pump depletion by the first signal. Clearly, the instability in BEFWM favors the first acoustic wave that is established. Although this experiment does not directly confirm the predictions of computer modeling, it lends support to the concept that, once established, the acoustic wave does not adapt to changes in the input signal.

Conclusions

We have measured the threshold for instability in BEFWM as a function of both the ratio of the pump beam intensities and the phase mismatch. The measured thresholds agree with theoretical modeling. Measurements of noise in BEFWM have also been made. The noise observed in BEFWM shows a factor-of-three increase over the noise observed in a simple amplifier operating under similar conditions. This increase is thought to be related to amplification of the second pump beam by the first pump beam. Competition between two signals with a relative time delay has also been investigated, and indicates that once the instability in the four-wave mixing process is established, it is self-sustaining and will not respond to changes in the input signal.

References

[1] N. F. Andreev, V. I. Bespalov, A. M. Kiselev, A. V. Matveev, G. A. Pasmanik, and A. A. Shilov, "Wavefront inversion of weak optical signals with a large reflection coefficient," *JETP Lett.*, vol. 32, pp. 625–629, 1981.

[2] V. I. Bespalov, E. L. Bubis, S. N. Kalugina, V. G. Manishin, A. V. Matveev, G. A. Pasmanik, P. S. Razenshtein, and A. A. Shilov, "Stimulated Brillouin scattering in a field of opposite light waves," *Sov. J. Quantum Electron.*, vol. 12, pp. 1544–1547, 1982.

[3] N. F. Andreev, V. I. Bespalov, M. A. Dvoretskii, and G. A. Pasmanik, "Four-wave hypersonic reversing mirrors in the saturation regime," *Sov. J. Quantum Electron.*, vol. 14, pp. 999–1000, 1984.

[4] A. M. Scott and M. S. Hazell, "High efficiency scattering in transient Brillouin enhanced four-wave mixing," *IEEE J. Quantum Electron.*, vol. QE-22, pp. 1248–1257, 1986.

[5] V. I. Bespalov, A. V. Matveev, and G. A. Pasmanik, "Limiting sensitivity of a stimulated-Brillouin-scattering amplifier and a four-wave hypersonic phase-conjugating mirror," *Radiophys. Quantum Electron.*, vol. 29, pp. 818–830, 1987.

[6] A. M. Scott and K. D. Ridley, "A review of Brillouin-enhanced four-wave mixing," *IEEE J. Quantum Electron.*, vol. 25, pp. 438–459, 1989.

[7] J. R. Ackerman and P. S. Lebow, "Output beam steering in a high reflectivity Brillouin enhanced four-wave mixing conjugator," *IEEE J. Quantum Electron.*, vol. 25, pp. 479–483, 1989.

[8] P. Narum, A. L. Gaeta, M. D. Skeldon, and R. W. Boyd, "Instabilities of laser beams counterpropagating through a Brillouin-active medium," *J. Opt. Soc. Amer. B*, vol. 5, pp. 623–628, 1988.

[9] W. Kaiser and M. Maier, "Stimulated Rayleigh, Brillouin and Raman spectroscopy," in *Laser Handbook*, vol. 2, F. T. Arrecchi and E. O. Shulz-Dubois, Eds. Amsterdam, The Netherlands: North Holland, 1972.

[10] A. I. Erokhin, V. I. Kovalev, and F. S. Faizullov, "Determination of the parameters of a nonlinear response of liquids in an acoustic resonance region by the method of nondegenerate four-wave interaction," *Sov. J. Quantum Electron.*, vol. QE-16, pp. 872–877, 1986.

[11] A. M. Scott, "Efficient phase conjugation by Brillouin enhanced four-wave mixing," *Opt. Commun.*, vol. 45, pp. 127–132, 1983.
[12] A. Z. Matveev, "Noise of thermal and hypersonic four-wave reversing mirrors and influence of wave mismatch," *Sov. J. Quantum Electron.*, vol. 17, pp. 466–472, 1987; ——, "Noise of four-wave hypersonic wavefront reversing mirrors under absolute instability conditions," *Sov. J. Quantum Electron.*, vol. 15, pp. 783–787, 1985; A. Z. Matveev and G. A. Pasmanik, "Noise in a wavefront-reversal system with a preliminary amplifier," *Sov. J. Quantum Electron.*, vol. 14, pp. 187–192, 1984.
[13] A. M. Scott, D. E. Watkins, and P. Tapster, "Gain and noise characteristics of a Brillouin amplifier and their dependence on the spatial structure of the pump beam," *J. Opt. Soc. Amer. B*, vol. 7, pp. 929–935, 1990.
[14] E. L. Bubis, O. V. Kulagin, G. A. Pasmanik, and A. A. Shilov, "Comparison between the efficiencies of stimulated Brillouin scattering in opposite directions in a field of complex conjugate pump beams," *Sov. J. Quantum Electron.*, vol. 14, pp. 815–817, 1984.
[15] N. F. Andreev, V. I. Bespalov, M. A. Dvoretskii, and G. A. Pasmanik, "Phase conjugation of single photons," *IEEE J. Quantum Electron.*, vol. 25, pp. 346–350, 1989.
[16] ——, "The limiting sensitivity on a four-wave hypersound WFR mirror coupled to a laser amplifier," *Izv. Akad. Nauk SSSR, Ser. Fiz.*, vol. 52, pp. 1205–1208, 1988; *Bull. Acad. USSR, Phys. Ser.*, vol. 52, no. 6, pp. 145–148, 1988.
[17] A. M. Scott and P. Waggot, "Phase conjugation by self pumped Brillouin induced four wave mixing," *Opt. Lett.*, vol. 12, pp. 835–837, 1987.

D. E. Watkins, photograph and biography not available at the time of publication.

Andrew M. Scott was born in Glasgow in October 1953. He received the B.Sc. degree from Edinburgh University and the Ph.D. degree from Hull University in 1981.

He joined the Royal Signals and Radar Establishment in 1980 and works on nonlinear optical phase conjugation.

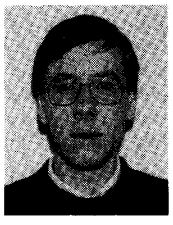

Kevin D. Ridley was born in England in 1965. He received the B.Sc. degree in applied physics from the University of Bath in 1987.

He joined the Royal Signals and Radar Establishment in 1987. His research interests are phase conjugation techniques and stimulated Brillouin scattering. He is currently working towards the Ph.D. degree as an external student at Imperial College, London.